David Tomás Sánchez Martínez
Lourdes García Rodríguez
(coordinadores)

Proceedings of the 7th International Seminar on ORC Power Systems

Editorial Universidad de Sevilla

Proceedings of the 7th International Seminar on

ORC
Power Systems

David Tomás Sánchez Martínez
Lourdes García Rodríguez
(coordinadores)

Proceedings of the 7th International Seminar on

ORC Power Systems

(ORC2023)

4th to 6th
SEPTEMBER
SEVILLE 2023

EDITORIAL UNIVERSIDAD DE SEVILLA

Sevilla, 2024

Colección Actas
Núm.: 91

Review chairs of the 7th Internation Seminar on ORC Power Systems

Prof. Christoph Wieland (University of Duisburg-Essen) - *Review Chair*
Prof. Sotirios Karellas (National Technical University of Athens) - *Review Co-Chair*
Prof. Teemu Turunen-Saaresti (LUT University) - *Review Co-Chair*
Dr. Diego-César Alarcón-Padilla (Plataforma Solar de Almería - CIEMAT) - *Review Co-Chair*
Dr. Francesco Crespi (Universidad de Sevilla) - *Review Co-Chair*

ISBN 978-84-472-2745-7
DOI: https://dx.doi.org/10.12795/9788447227457

Diseño de cubierta y maquetación: los autores

INDEX OF CONTRIBUTIONS

DOI: https://dx.doi.org/10.12795/9788447227457_84

MAPPING THE TECHNO-ECONOMIC POTENTIAL OF NEXT-GENERATION CSP PLANTS RUNNING ON TRANSCRITICAL CO_2-BASED POWER CYCLES

Pablo Rodríguez-deArriba[1,*], Francesco Crespi[1], Sara Pace[2], David Sánchez[1]

[1] *University of Seville, Department of Energy Engineering, Camino de los descubrimientos s/n, 41092, Seville, Spain*
[2] *Politecnico di Milano, Department of Energy, Via Lambruschini 4, 20156, Milan, Italy*

[*]Corresponding Author: prdearriba@us.es

ABSTRACT

Although the thermodynamic potential of transcritical/supercritical CO_2-based power cycles for next generation Concentrated Solar Power plants has been already confirmed in literature, further investigation to assess the actual feasibility of this technology from a techno-economic standpoint is needed. In fact, large uncertainty is found when it comes to the estimation of the CAPEX and OPEX of the power block, and the same can be said for the solar subsystem when high Turbine Inlet Temperatures are considered (>700 ºC).
Bearing this in mind, this paper presents a methodology to map the techno-economic potential of next-generation Concentrated Solar Power plants running on CO_2-based mixtures, with the final aim to identify the threshold (breakeven) costs of the main subsystems enabling a clear gain in terms of Levelised Cost of Electricity with respect to state-of-the-art steam-based CSP.
Two different systems are studied which differ in the composition and peak temperature of the Heat Transfer Media: a SoA molten salts system operating at a TIT of 550 ºC (Gen I) and a solid particle system with TIT=700 ºC (Gen II). An integrated platform able to simulate all CSP plant subsystems and perform hourly calculations is built in Matlab employing Artificial Neural Networks to simulate the solar field, ensuring extremely high computational speed.
To overcome the high uncertainty in terms of cost estimation, a two-step analysis is developed: firstly, the CAPEX of the entire plant is calculated assuming correlations from literature, except for the power block, whose estimate brings about the largest uncertainty. As a result, the minimum power block cost allowing a LCoE lower than a certain target is identified. Secondly, an inverse methodology is applied, setting the power block cost and assessing the minimum CAPEX of the solar subsystem. As a result, a map is obtained showing the target CAPEX to be accomplished by sCO_2+CSP if a clear reduction of the LCoE of this technology is to be achieved.

1 INTRODUCTION

Concentrated Solar Power (CSP) plants combined with supercritical carbon dioxide (sCO_2) power cycles are widely believed to be a key-enabler of the complete decarbonisation of the power generation sector. This is due to the combination of various outstanding features of this technology, such as the high thermal efficiency, low footprint and high operational flexibility -notable features attributed to sCO_2 power cycles- as well as high dispatchability, brought by the use of Thermal Energy Storage (TES). This last feature stems as a major advantage over variable renewable energy sources such as photovoltaics and wind. Nevertheless, the cost-effectiveness of CSP+sCO_2 is still unclear, and further investigation is needed to reduce the Levelised Cost of Electricity (LCoE) of this technology in order to make it truly competitive in the energy market. In this regard, the SCARABEUS project aims to reduce the LCoE of CSP plants located in areas with high solar resource and high annually-averaged ambient temperature. To achieve this, the project investigates the use of innovative power cycles based on CO_2 mixtures that can attain higher thermal efficiency than supercritical CO_2 and steam cycles (Crespi *et al.*, 2022 (b)).

Bearing this in mind, two CO_2-based CSP plants at two different Turbine Inlet Temperature (TIT) levels, 550 ºC (Gen I) and 700 ºC (Gen II), are compared. Gen I uses conventional solar subsystem technology based on Solar Salt as Heat Transfer Media (HTM) coupled with two-tank TES, whereas Gen II is based on free-falling particle receivers (FFPR). A Matlab-based computational platform is developed to calculate the annual electricity production for different Solar Multiple (SM) and TES capacities. A two-step analysis is employed to overcome the high uncertainty in cost estimation: i) in the first step, the CAPEX of the entire plant is calculated using correlations taken from literature for all subsystems except the power block, which is the section of the plant with larges uncertainty. The minimum cost of the power block necessary to achieve the target LCoE (100 $/MWh) -an arbitrary upper limit set according to the objectives of the SCARABEUS project (Binotti *et al.*, 2020)- is then identified for each case; ii) in the second step, an inverse methodology is used to set the cost of the power block and to assess the minimum CAPEX of the solar subsystem accordingly, with the final aim of mapping the target CAPEX that needs to be achieved by sCO_2+CSP to reduce LCoE below state-of-the-art (SoA) technologies based on steam turbines.

2 COMPUTATIONAL ENVIRONMENT

A Matlab-based computational platform has been developed to perform annual plant simulations. The platform comprises four main modules: solar field, solar receiver, TES and power block. Additionally, certain assumptions are made for the calculation of auxiliary loads (i.e., heliostat tracking, heliostat start-up and HTM conveyance). It is worth noting that the technology and models used are specific to each generation considered (Gen I or Gen II), each of which blocks will be further detailed in the following subsections. The hourly calculation flowchart has been adapted from González-Portillo *et al.* (2021). Calculations apply to a plant located in Seville (Spain), with design Direct Normal Irradiance and ambient temperature corresponding to the 95th percentile of the annual distribution: 840 W/m^2 and 36 ºC. The annual direct irradiance is 1773 kWh/m^2·year. **506**

2.1 Solar field

The SolarPILOT software is employed to simulate the solar field (Wagner and Wendelin, 2018). For Gen I, the solar field is a circular surrounding field with an external cylindrical receiver atop the central tower. For Gen II, free-falling, cavity-type particle receivers (FFPR) are used, making it not feasible to employ surrounding fields; North-fields are used instead. This approach, however, poses a significant challenge for utility-scale plants (≥100 MW) in terms of land utilisation and, moreover, inefficient optical performance, inasmuch as heliostats that are further from the tower perform poorly from an optical standpoint. As a solution, multi-receiver designs, with more than one receiver in the same tower, are studied. In this work, a design with three FFPRs -facing North, East and West- is considered, as proposed in (Mills *et al.*, 2022); the particular specifications to simulate the multi-FFPR design in SolarPILOT can be retrieved from the works by González-Portillo *et al.* (2021) and Mills *et al.* (2022). With the objective of simplifying the integration of SolarPILOT within the integrated platform and of significantly increasing the computational speed when studying different solar field configurations, a surrogate model based on Artificial Neural Networks was created using Matlab's Deep Learning Toolbox. First, a training dataset of 1000 elements was generated, where each sample represents a feasible design of the solar field -randomly generated by varying the design degrees of freedom- whose performance is evaluated for a random position of the sun selected from a set of equally spaced positions based on declination angle (Wagner, 2008). The Levenberg-Marquardt algorithm was used to train the neural networks, and a sensitivity analysis was conducted on the number of neurons in the hidden layer. As a result, an Artificial Neural Network capable of estimating the solar field's optical efficiency for a given design (specified by the number of heliostats, tower height, and receiver area) and operating conditions (determined by Direct Normal Irradiance and sun position) was created. For multi-receiver designs, the ANN also provides the fraction of thermal power incident on each of the three receivers. The estimation of optical efficiency yields a Root Mean Square Error of 0.82 and 2.3 percentage points, respectively, indicating the higher computational complexity of the second system compared to the former. Future research should concentrate on thoroughly examining and enhancing the training process, reducing training errors, and investigating the impact of uncertainty on the final results.

2.2 Solar receiver

External receivers similar to those employed in SoA CSP plants are used for Gen I, where Solar Salt (60%$NaNO_3$-40%KNO_3) is the HTM used in the receiver and TES. Molten salts are heated up from 387.9 ºC to 565 ºC in the receiver, whose thermal performance is simulated with the System Advisor Model (SAM). The design of the receiver includes size, number of panels, number of tubes, and thickness and is assumed constant throughout the study for the sake of simplicity.

In the multi-receiver design of Gen II, particles fall through the receiver by gravity and are heated directly by the solar radiation that enters the cavity (Ho *et al.*, 2016). *CARBO Accucast ID50* particles with a diameter of 350 µm are considered, and the thermophysical properties are taken from the work by Ho *et al.* (2017). Particles enter the receiver at 600 ºC and are heated up to 800 ºC. As a further simplification, all three receivers are assumed to have an aspect ratio of 1 and the same aperture area, and the aperture and curtain areas are considered to be equivalent (Mills *et al.*, 2022). The performance of the FFPR is estimated with the model proposed by González-Portillo *et al.* (2021). As a result of a preliminary analysis, it is decided to employ a constant FFPR particle curtain size of 18x18 m.

2.3 TES

A ground-based Thermal Energy Storage system (TES) composed of two cylindrical tanks is considered for both Gen I and Gen II, employing molten salts in the former and solid particles in the latter. The height-to-diameter ratio is set to 0.5 and 2 for molten salts in Gen I and for particles in Gen II, respectively. A dead volume of 20 % is assumed for both systems. The thermal losses are calculated assuming a thermal resistance of 4 m^2K/W, taken from González-Portillo *et al.* (2021).

2.4 Power subsystem

507

The power subsystem includes three modules: power cycle, heat rejection unit and primary heat exchanger (PHX). The power cycle used in this system is a transcritical cycle running on a binary mixture of 80%CO_2-20%SO_2 (molar basis), whose detailed description can be found in previous publications by the authors (Crespi *et al.*, 2022 (a), Crespi *et al.*, 2022 (b), Rodríguez-deArriba *et al.*, 2022). A modular air-cooled heat exchanger with induced-draft axial fans is used to condense the mixture, thus minimising water consumption of the plant. The final design uses multiple units equipped with three axial fans each, two of them with single-speed drives and the other one with a variable frequency drive. This choice is considered a promising trade-off between enhanced performance and moderate capital cost increase (more info in Rodríguez-deArriba *et al.*, 2023b). Further research is needed to determine the optimal number of VFDs though. The primary heat exchangers in Gen I and Gen II are different. For Gen I, a shell-and-tube heat exchanger with molten salts on the shell side and the working fluid flowing inside the tubes is employed. For Gen II, a particle-to-working fluid moving packed-bed shell-and-tube heat exchanger is used; for a detailed description of this component and a comparison with other existing technologies, the readers may refer to the work by Ho *et al.* (2019).

The power cycle is modelled in Thermoflex environment, modified with a series of user-defined modules to enable the simulation of SCARABEUS-specific components. The air-cooled heat exchanger is modelled in Matlab, as explained in past works by partners of the consortium (Illýes *et al.*, 2022, Rodríguez-deArriba *et al.*, 2023a), while a numerical code for the particle-to-working fluid shell-and-tube heat exchanger is also specifically developed in the same environment to design and simulate this component. To calculate the total conductance UA, the heat exchanger has been modelled as a cross-flow heat exchanger. The heat transfer coefficient on the CO_2 side has been determined using Gnielinski's correlation whereas that on the (dominating) particle side is implemented following the simplified heat transfer model presented in Hertfel and Zunft (2022). Table 1 compares the main design parameters for the power subsystem of Gen I and Gen II. In this regard, cycle thermal efficiency refers to the ratio from gross power output to heat input to the cycle. On the other hand, net efficiency refers to the ratio from net power output of the power block to total heat input into the PHX. When calculating net power output, several factors are considered, including losses in the electric motor and generator, auxiliary power consumption of the air-cooled condenser, and power consumed by the HTM conveyance system from the hot tank to the cold tank through the PHX.

Table 1. Power subsystem design parameters for Gen I and Gen II

Parameter	**Gen I**	**Gen II**
Turbine inlet temperature [ºC]	550	700
Minimum cycle temperature [ºC]	50	50
Gross power output [MW]	100	100
Cycle thermal efficiency [%]	44.1	51.05
Air-cooled condenser fan power [kWe]	1181	885.0
PHX power consumption [kWe]	239.7	116.6
Net power output [MWe]	90.96	92.43
Net efficiency [%]	40.1	47.1

The CSP plant is assumed to operate in base load, thus keeping net power output as close to the rated value as possible. Accordingly, the effect of part-load operation is disregarded in this work, which accounts for the impact of variable ambient temperature only. Figure 1 shows the net output (a) and net efficiency (b) of the power subsystem as a function of ambient temperature for Gen I and Gen II. For ambient temperatures lower than design, the power block operates at its design point with reduced auxiliary power consumption of the air-cooled condenser; this results in a slightly higher net power output and efficiency. For ambient temperatures higher than the rated value, the air-cooled heat exchanger is not able to condense the working fluid at the rated condensation pressure, and this pressure must be increased, resulting in a higher minimum cycle temperature. However, doing so also requires decreasing TIT to keep the return temperature of HTM (i.e., temperature at the outlet from the PHX) equal to its design value. All this results in a drastic drop in both net power and efficiency.

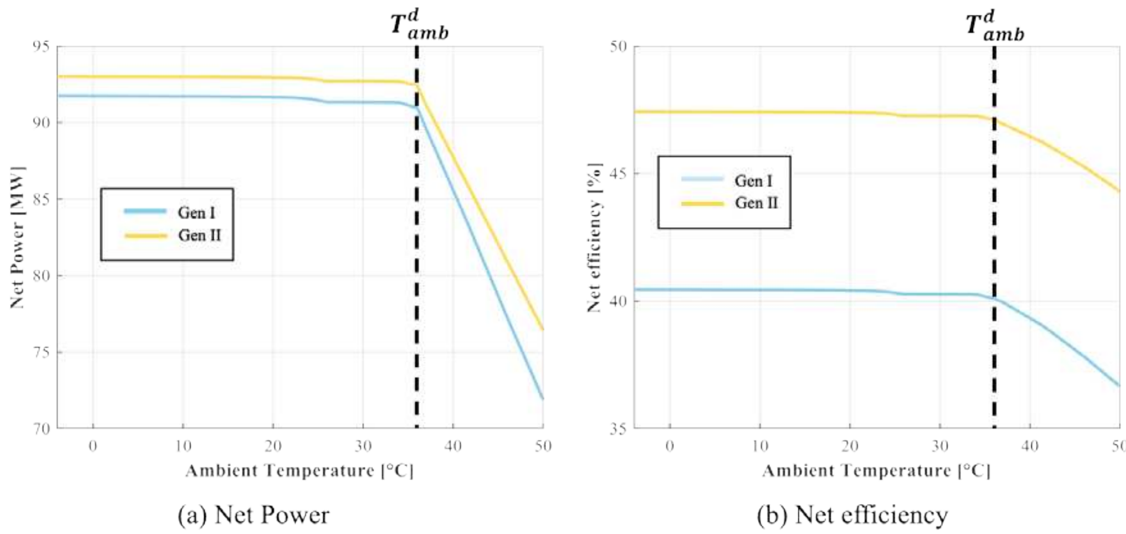

(a) Net Power (b) Net efficiency

Figure 1. Power subsystem: (a) net power and (b) net efficiency as a function of ambient temperature

2.5 Cost models

Two scenarios are considered for the solar field and site preparation costs: 140 $/m^2, representative of SoA plants (Manzolini *et al.*, 2021), and 60 $/m^2, corresponding to future projections taken from the work by Murphy *et al.* (2019). The costs of the tower and receiver in Gen I are taken from Manzolini *et al.* (2021). The latter cost is then replaced by the costs reported by González-Portillo *et al.* (2021), for the FFPR, particle lifts and particle-based TES system in a Gen II plant. The TES based on Solar Salt is calculated using an in-house tool adapted from past work by some of the authors (Rodríguez *et al.*, 2016), resulting in a specific cost of 38.2 $/kWh. All cost estimates refer to 2020$.

It is to note that, given the lack of reliable cost correlations for the components of a power block running on CO_2 mixtures, the direct calculation of the power block cost is not addressed in this paper. Rather, this cost is reverse-calculated in order to attain the target cost of energy. The additional parameters necessary for the economic assessment are presented in Table 2, taken from González-Portillo *et al.* (2021).

Table 2. Assumptions of the economic assessment

Parameter	**Value**
Plant lifetime	30 year
Discount rate	7 %
Inflation	2.5 %
Contingency Cost	10 %
Construction Cost	9 %
Land cost	2.47 $/m²$
Fixed O&M Cost	40 $/kW·year
Variable O&M Cost	0.003 $/kWh

3 RESULTS

3.1 Annual Energy Production and reference case

The computational platform described in earlier sections is used to calculate the annual yield of both Gen I and Gen II power plants. A sensitivity analysis is also conducted, varying the number of heliostats (through Solar Multiple, SM) and energy storage capacity (equivalent hours of storage, h_{TES}). The results are shown in Figure 2. It is observed that, for the same number of heliostats and h_{TES}, the Gen I system is able to produce slightly more electricity than the Gen II system. This is because, for the same number of heliostats (i.e., same total reflective area), the surrounding field in Gen I attains higher optical efficiency than the multi-receiver field in Gen II. This data is used to create a spline-fitting surface in Matlab, which is used in the next sections to interpolate the annual production of energy for any intermediate values of SM and h_{TES}.

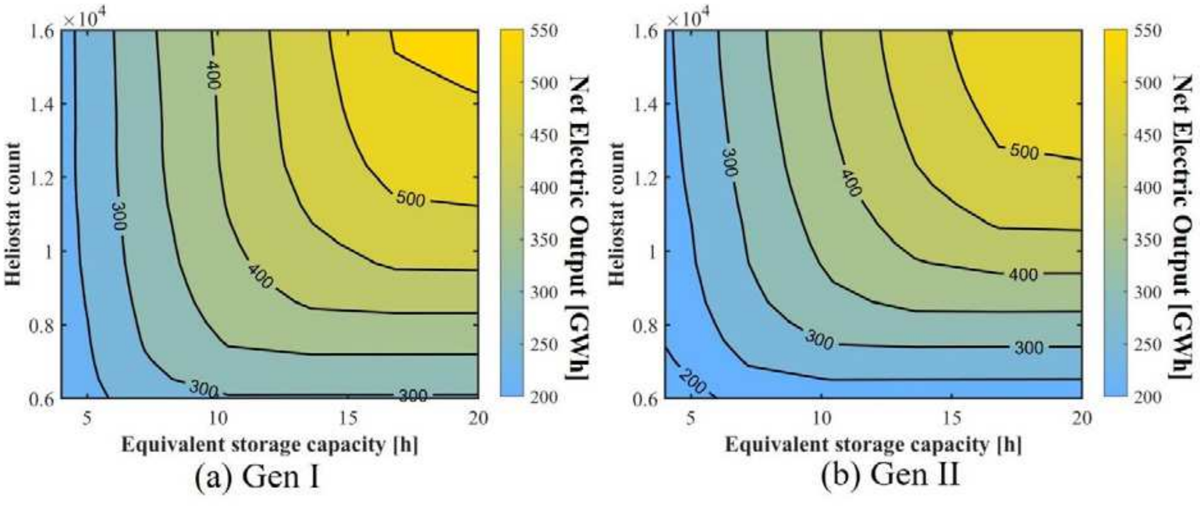

Figure 2. Net electric output as a function of number of heliostats and TES capacity for (a) Gen I and (b) Gen II

For each generation, a reference case is selected, assuming optimised values for the number of heliostats and storage capacity: 11070 heliostats (SM 3.26) and 17 hours for Gen I, 11800 (SM 3.42) and 18.2 hours for Gen II. Interestingly, in spite of the worse optical and thermal performances of the solar field and receiver in Gen II, the corresponding optimum number of heliostats is very similar to that of Gen I. This is because this lower performance is compensated for by the higher net efficiency of the power block of Gen II in terms of global efficiency. As a consequence, the cost of the solar field is similar in both systems, as observed from a breakdown of specific costs provided in Figure 3.

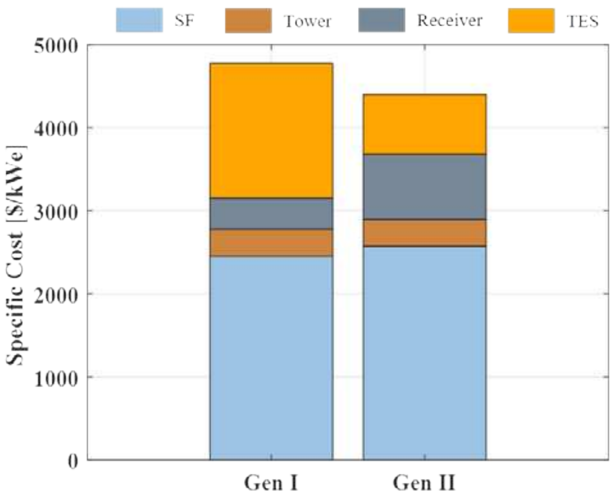

Figure 3. Cost breakdown of the solar subsystem for Gen I and Gen II cases.

The tower costs are identical in both cases, since both make use of a 218 m tower (Gasa *et al.*, 2022). Nevertheless, the multi-receiver system using FFPRs is twice as expensive as the external receiver system in Gen I. In addition to the fact that three receivers are needed in the particle-based solar subsystem, this is also due to the need for a costly particle-elevator system (González-Portillo *et al.*, 2022). Finally, a higher than 50 % cost reduction of the TES system is observed when switching from molten salt storage (Gen I) to particle storage (Gen II). This result is noteworthy since it addresses one of the primary challenges highlighted in literature with regards to the integration of CO_2-based systems with conventional TES based on molten salts: the important increase in cost with respect to the TES employed in SoA steam turbine-based CSP plants, owing to the lower temperature difference between hot and cold tanks. 510

3.2 Optimization of power subsystem cost

In this section, the impact of the power subsystem cost is assessed by means of a sensitivity analysis to its specific cost. For each point of the sensitivity analysis, the solar multiple and the storage capacity are optimised in order to minimise LCoE, using the cost functions for the solar subsystem elements described in the previous section.

Results for both Gen I and Gen II are presented in Figure 4, for the current and future solar field cost scenarios. Firstly, it is worth noting that, regardless of the generation and solar field cost considered, both Gen I and Gen II achieve significantly lower LCoE than 167 $/MWh, a value representative of a CSP plant based on steam turbine and two-tank molten salt TES located in Seville (Manzolini *et al.*, 2021). This highlights the potential of the SCARABEUS concept to reduce the cost of CSP technology. Moreover, it is observed that, considering current SF cost values, the LCoE target of 100 $/MWh (see introduction) can be achieved by any of the two generations of SCARABEUS if the specific capital cost of the power block is below 1700-1800 $/kWe.

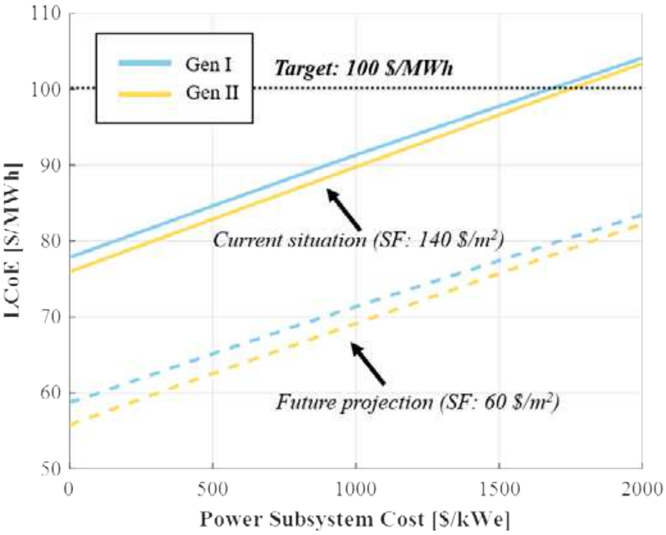

Figure 4. Minimum LCoE [$/MWh] achievable as a function of Power Subsystem Cost [$/kWe]

The results in the foregoing paragraph set an upper limit that the SCARABEUS technology must not exceed in order to yield an LCoE lower than 100 $/MWh. This threshold seems to be achievable in practice, considering that the specific cost of the power block of a SoA steam-based CSP plant is around 1400 $/kWe (Manzolini *et al.*, 2021), and the cost of a supercritical CO_2 recompression cycle is estimated at ~1000 $/kWe (Ho *et al.*, 2016). Assuming that the cost of the technology studied here is similar to that using pure sCO_2, an LCoE~90 $/MWh is to be expected.

Interestingly, Gen I and Gen II perform rather similarly in terms of LCoE, with differences in the range of 0.5-3.5 $/MWh. Thus, even if this result can be affected by the large uncertainty in cost estimation for Gen II, brought about by the very low TRL of this technology, this might suggest that the best path to develop a next-generation CSP is not achieving extremely high TIT (>700 ºC) but, rather, optimising the cycles for intermediate (moderately high) TITs, for which TES based on molten salts are still feasible (≃600 ºC). 511

Finally, it is worth highlighting that, even if the cost of the power subsystem were zero, there exists a minimum LCoE of around 75-80 $/MWh that the technology cannot exceed, whose exact value depends on the selected location. Regarding the two scenarios of solar field costs, it is observed that if the future projection is met, LCoE would be reduced by 20 $/MWh regardless of the power subsystem cost.

3.3 Minimum solar subsystem cost

Calculating the cost of the solar subsystem is subject to a significant uncertainty as well. Figure 5 presents a mapping of the technology based on the specific cost of the solar and power subsystems, along with iso-lines of constant LCoE. This map allows to set target costs for the SCARABEUS technology based on the desired LCoE or, equivalently, to determine the resulting LCoE for given costs of both subsystems. The figure was generated assuming the reference values of SM and h_{TES} for each generation and for contemporary solar field costs. The total capital cost for a specific LCOE can be calculated by adding the power subsystem cost (x-axis) and solar subsystem cost (y-axis). This value is constant along any iso-LCoE line. Furthermore, the total capital cost evolves linearly with the LCOE. For instance, to achieve a reduction in LCOE from $120/MWh to $60/MWh, the total capital cost should decrease from 7899 $/kWe to 3424 $/kWe for Gen I, and from 7596 $/kWe to 3235 $/kWe for Gen II.

Two grey bands are added, estimating the cost of the solar subsystem according to the correlations from literature. The upper band represents the current costs of the solar field (120 $/m²) whereas the lower band applies to future projections (60 $/m²). For each band, the upper boundary corresponds to the solar subsystem cost of Gen I while the lower boundary corresponds to Gen II. Interestingly, an increase in the solar subsystem cost for higher costs of the power subsystem are observed (i.e., the bands become wider for higher power block costs). This is explained by the larger size of both the solar field and thermal energy storage system that aims to increase the annual yield of the plant in order to compensate for the higher cost of the power subsystem. Also, it is observed that this phenomenon is more pronounced for Gen I (upper limit of the bands) due to the higher specific cost of the molten salt storage system.

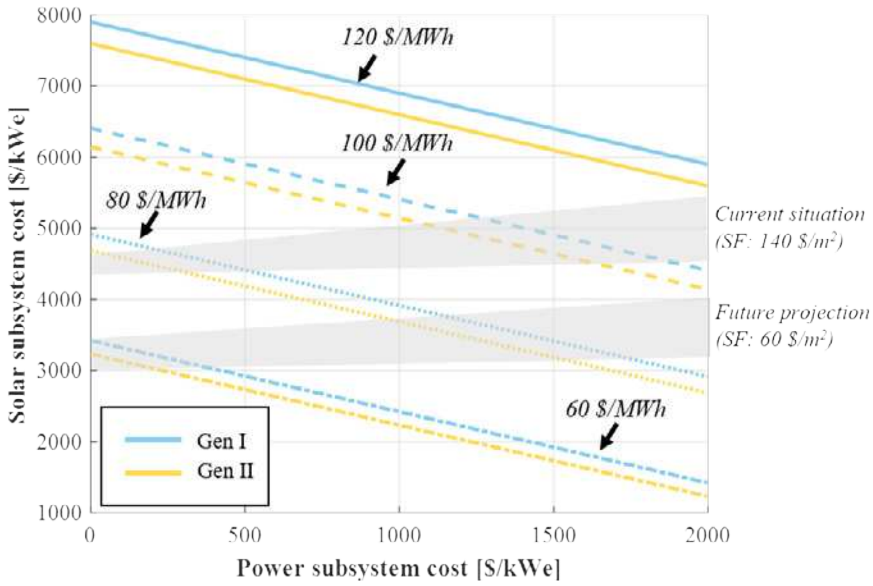

Figure 5. Constant-LCoE lines for different combinations of solar and power subsystem costs (blue for Gen I and yellow for Gen II). Labels report LCoE associated to each line set [$/kWe]

The graphical results presented in this section confirm the tight link between the cost of the power and solar subsystems, and the dominant effect of the latter over the former (moderate slope of the constant LCoE lines). From a practical standpoint, the results also confirm that achieving a much lower LCoE than SoA CSP plants based on steam turbines is within reach of the SCARABEUS technology, either with contemporary CO_2-mixture technology (Gen I) or with more advanced components (Gen II). There is of course uncertainty inherent to this analysis but the fact that the methodology adopted works upstream to determine breakeven costs from the target LCoE rather than downstream from the estimated values of different subsystems reduces this uncertainty to a large extent.

4 CONCLUSIONS

In this study, the utilisation of transcritical power cycles based on CO_2 mixtures in CSP plants has been evaluated from a techno-economic standpoint. Two CSP plant schemes using different receiver technology have been compared: conventional molten salt receivers with a maximum temperature of 565 ºC (Gen I) and solid particle receivers with a maximum temperature of 800 ºC (Gen II).

It is concluded that:

- Both systems can potentially achieve LCoE’s lower than 100 $/MWh for a reference plant in Seville, as long as the cost of the power subsystem is not higher than 1700 $/kWe. The specific cost of the power subsystem is expected to be lower than that of SoA CSP plants based on steam turbines (1400 $/kWe) due to the lower footprint.
- The resulting LCoE for Gen I and Gen II is very similar, slightly lower for Gen II thanks to the significant cost reduction of the TES system.
- If the specific cost of the solar field were to decrease according to projections from literature, LCoE’s in the area of ~70 €/MWh would be within reach for the SCARABEUS concept for a reasonably good location (not necessarily optimum).

However, it must be highlighted that cost estimates for the receiver technology used in Gen II are subject to higher uncertainty. Therefore, future work should address the estimation of the cost of the power block technology, as well as study the uncertainty in cost estimates, especially for the technology used in Gen II. Moreover, the economic performance could be further improved through a simultaneous, joint optimisation of the power cycle and solar subsystem. These efforts will allow for a more robust and accurate evaluation of the potential of SCARABEUS technology in the future power generation sector.

NOMENCLATURE

CAPEX	Capital Expenditure	LCoE	Levelised Cost of Electricity
CSP	Concentrated Solar Power	PHX	Primary Heat Exchanger
FFPR	Free-falling particle receiver	SM	Solar Multiple
Gen	Generation of CSP plant	SoA	State-of-the-art
h_{TES}	Equivalent hours of storage	TES	Thermal Energy Storage
HTM	Heat Transfer Media	TIT	Turbine Inlet Temperature

REFERENCES

Binotti, M. et al. (2020) 'SCARABEUS: Supercritical carbon dioxide/alternative fluid blends for efficiency upgrade of solar power plants', in. *SOLARPACES 2019: International Conference on Concentrating Solar Power and Chemical Energy Systems*, Daegu, South Korea, p. 130002. Available at: https://doi.org/10.1063/5.0028799.

(a) Crespi, F. *et al.* (2022) 'Preliminary investigation on the adoption of CO 2 -SO 2 working mixtures in a transcritical Recompression cycle', *Applied Thermal Engineering*, 211, p. 118384. Available at: https://doi.org/10.1016/j.applthermaleng.2022.118384.

(b) Crespi, F. *et al.* (2022) 'Thermal efficiency gains enabled by using CO2 mixtures in supercritical power cycles', *Energy*, 238, p. 121899. Available at: https://doi.org/10.1016/j.energy.2021.121899.

Gasa, G. *et al.* (2022) 'Life cycle assessment (LCA) of a concentrating solar power (CSP) plant in tower configuration with different storage capacity in molten salts', *Journal of Energy Storage*, 53, p. 105219. Available at: https://doi.org/10.1016/j.est.2022.105219.

González-Portillo, L.F., Albrecht, K. and Ho, C.K. (2021) 'Techno-Economic Optimization of CSP Plants with Free-Falling Particle Receivers', *Entropy*, 23(1), p. 76. Available at: https://doi.org/10.3390/e23010076.

González-Portillo *et al.* (2022). Sensitivity Analysis of the Levelized Cost of Electricity for a Particle-Based Concentrating Solar Power System. *Journal of Solar Energy Engineering*, 144(3), 030902. Available at https://doi.org/10.1115/1.4053167.

Hertel, J.D. and Zunft, S. (2022) 'Experimental validation of a continuum model for local heat transfer in shell-and-tube moving-bed heat exchangers', Applied Thermal Engineering, 206 p. 118092. Available at: https://doi.org/10.1016/j.applthermaleng.2022.118092.

Ho, C.K. *et al.* (2016) 'Technoeconomic Analysis of Alternative Solarized s-CO2 Brayton Cycle Configurations', *Journal of Solar Energy Engineering*, 138(5), p. 051008. Available at: https://doi.org/10.1115/1.4033573.

Ho, C.K. *et al.* (2017) 'Characterization of Particle Flow in a Free-Falling Solar Particle Receiver', *Journal of Solar Energy Engineering*, 139(2), p. 021011. Available at: https://doi.org/10.1115/1.4035258.

Ho, C.K. *et al.* (2019) 'Evaluation of Alternative Designs for a High Temperature Particle-to-sCO2 Heat Exchanger', *Journal of Solar Energy Engineering*, 141(2), p. 021001. Available at: https://doi.org/10.1115/1.4042225.

Illyés, V. *et al.* (2022) 'Design of an Air-Cooled Condenser for CO2-Based Mixtures: Model Development, Validation and Heat Exchange Gain with Internal Microfins', in *Volume 9:*

513

Supercritical CO2. ASME Turbo Expo 2022: Turbomachinery Technical Conference and Exposition, Rotterdam, Netherlands: American Society of Mechanical Engineers, p. V009T28A016. Available at: https://doi.org/10.1115/GT2022-82438.

Manzolini, G. *et al.* (2021) 'A two-step procedure for the selection of innovative high temperature heat transfer fluids in solar tower power plants', *Renewable Energy*, 177, pp. 807–822. Available at: https://doi.org/10.1016/j.renene.2021.05.153.

Mills, B. *et al.* (2022) *Technoeconomics of Particle-based CSP Featuring Falling Particle Receivers with and without Active Heliostat Control*. SAND2022-13437, 1890267, 710418, pp. SAND2022-13437, 1890267, 710418. Available at: https://doi.org/10.2172/1890267.

Murphy, C., et al. (2019). The potential role of concentrating solar power within the context of DOE's 20230 solar cost targets. Retrieved from https://www.osti.gov/servlets/purl/1506623

Rodríguez, J.M. *et al.* (2016) 'Techno-economic assessment of thermal energy storage solutions for a 1 MWe CSP-ORC power plant', *Solar Energy*, 140, pp. 206–218. Available at: https://doi.org/10.1016/j.solener.2016.11.007.

Rodríguez-deArriba, P. *et al.* (2022) 'The potential of transcritical cycles based on CO2 mixtures: An exergy-based analysis', *Renewable Energy*, 199, pp. 1606–1628. Available at: https://doi.org/10.1016/j.renene.2022.09.041.

(a) Rodríguez-deArriba, P. *et al.* (2023). 'A methodology to design air-cooled condensers for supercritical power cycles using carbon dioxide and carbon dioxide mixtures'. In: *Proceedings of the 5th European sCO_2 Conference for Energy Systems*. Available at: https://doi.org/10.17185/duepublico/77329.

(b) Rodríguez-deArriba, P. *et al.* (2023). 'Assessment of part-load operation strategies of supercritical power cycles using carbon dioxide mixtures in CSP plants, including air-cooled condenser optimisation', in: *Proceedings of ASME Turbo Expo 2023,* Boston, USA.

Wagner, M.J. (2008) 'Simulation and predictive performance modeling of utility-scale central receiver system power plants'. (Doctoral dissertation). University of Wisconsin, Madison. Retrieved from http://digital.library.wisc.edu/1793/45001

Wagner, M.J. and Wendelin, T. (2018) 'SolarPILOT: A power tower solar field layout and characterization tool', *Solar Energy*, 171, pp. 185–196. Available at: https://doi.org/10.1016/j.solener.2018.06.063. **514**

ACKNOWLEDGEMENTS

The SCARABEUS project has received funding from the European Union's Horizon 2020 research and innovation programme under grant agreement Nº814985.

The Spanish Ministry of Universities is gratefully acknowledged for sponsoring the contract of Pablo Rodríguez de Arriba via FPU (Formación de Profesorado Universitario). Grant reference FPU21/04892.

This book contains the compilation of works contributed to the *7th International Seminar on Organic Rankine Cycle Power Systems* (ORC 2023), held in Seville between the 4th and 6th of September 2023. The event was hosted by Universidad de Sevilla on behalf of the Knowledge Centre on Organic Rankine Cycle Technology (KCORC), incorporated in The Netherlands.

The ORC conference, organized biennially, stems as the only conference that is specific to ORC technology, therefore gathering a diverse community whose affiliation spans across all the interested stakeholders, not only in this particular technology but also and in a broader context, in the energy transition. Original equipment manufacturers, professional associations, end-users, investors, policy makers, academics, scientists feel at home at ORC 2023.

The almost 100 proceedings in this book cover a wide variety of topics, from fundamentals to system integration through component design, accounting for thermodynamic performance as well as component design. In addition to this, and as a new track in 2023, works on heat pump technology were also accepted in order to raise awareness of the strong ties between both technologies, specifically in energy storage applications.

This book provides an excellent overview of the current maturity of power systems based on Organic Rankine Cycle technology for applications as diverse as geothermal and waste heat recovery in industry or downstream of other prime movers (e.g., marine applications). It is also an excellent source of information to understand the current challenges faced by the technology, stemming from a very competitive market and increasingly stringent environmental regulations.

The organizers of ORC 2023 hope that the reader finds this work as exciting as the attendees to the conference and, maybe, make the decision to join the 8th edition to the conference in 2025.

KCORC
KNOWLEDGE CENTER
ORGANIC RANKINE CYCLE

eUS EDITORIAL
UNIVERSIDAD DE SEVILLA